Dileptons and photons from central heavy-ion collisions at CERN-SPS

B. Kämpfer[a]FZR]Forschungszentrum Rossendorf, PF 510119, D-01314 Dresden, Germany*, K. Gallmeister[b][FZR]†, O.P. Pavlenko[c][FZR][d]ITP] Institute for Theoretical Physics, 252143 Kiev - 143, Ukraine and C. Gale[e]

[a][

[d][

[e] Physics Department, McGill University, Montreal, QC, H3A 2T8, Canada

A unique parameterization of secondary (thermal) dilepton and photon yields in heavy-ion experiments at CERN-SPS is proposed. Adding those thermal yields to background contributions the spectral shapes of the CERES/NA45, NA38, NA50, HELIOS/3 and WA98 data from experiments with lead and sulfur beams can be well described.

1. INTRODUCTION

Electromagnetic radiation represents penetrating probes mapping out the full space-time history of strongly interacting matter in the course of heavy-ion collisions. Particularly interesting is the stage of maximum temperature, where a quark-gluon plasma might be formed. Various properties of the quark-gluon plasma are calculable from first principles exploiting numerical lattice QCD techniques. The results, such as thermodynamical properties, can be interpreted within quasi-particle models [1]. Other quantities, such as the electromagnetic emission rates, are accessible within perturbation theory [2].

The motivation to measure electromagnetic signals in ultralrelativistic heavy-ion collisions is based on the hope to have a direct access to the hottest and densest stages of matter (cf. [3]). According to the present understanding of the dynamics of central heavy-ion collisions at CERN-SPS, the temperature range covered is $T_c \pm 50$ MeV (where $T_c \approx 170$ MeV is the confinement temperature). In this regime the electromagnetic emission rates from deconfined and confined hadronic matter are fairly similar (cf. [4,5]). Indeed, taking into account the empirical electromagnetic formfactors from the reaction $e^+e^- \to hadrons$ and including vector - axial vector mixing [6] one gets a dilepton rate which coincides with the lowest-order $q\bar{q}$ rate for invariant masses $M \geq 1.1$ GeV [5]. Below 1.1 GeV the dilepton spectrum of hadronic matter is determined by the sharp ϕ and ω peaks and the broad ρ peak. Hadronic reactions broaden the ρ peak so much that the net dilepton spectrum again resembles that from the $q\bar{q}$ rate down to $M \approx 300$ MeV [7]. It is therefore tempting to entirely describe the spectra at $M > 300$ MeV by the lowest-order $q\bar{q}$ rate, thus treating it as a convenient parameterization. Analog arguments

*Supported by BMBF grant 06DR921.
†Presently at University Giessen, Germany.

are not available for the real photon rate. Therefore, we use as a working hypothesis the lowest-order Born rates of the processes $q\bar{q} \to \gamma g$ and $qg \to \gamma g$ for thermal photons.

Many hadron observables at CERN-SPS energies can be described by thermal models. In line with this finding we will describe the secondary real and virtual photons by a thermal source which adds to the Drell-Yan-like yields and hadron decay contributions (hadronic cocktail and correlated semi-leptonic decays of open charm mesons).

2. ANALYSES OF EXPERIMENTAL DATA

By now the following experimental data are available: (i) lead beam at 158 A·GeV and Au, Pb targets: CERES (low-mass e^+e^-), NA50 (intermediate-mass $\mu^+\mu^-$), WA98 (direct photons), (ii) lead beam at 40 A·GeV and Au target: CERES (low-mass e^+e^-), (iii) sulfur beam at 200 A·GeV and Au, U, W targets: CERES (low-mass e^+e^-), NA38 (intermediate-mass $\mu^+\mu^-$), HELIOS/3 (low- and intermediate-mass $\mu^+\mu^-$), WA80 (upper bounds on direct photons). In addition, data with proton beams at these energies and also 450 GeV for various target nuclei are at our disposal.

2.1. A simple parameterization of the thermal source

The lowest-order rates are in Boltzmann approximation

$$\frac{dN_{\gamma *}}{d^4x d^4Q} \propto \exp\left\{-\frac{Q\cdot u}{T}\right\}, \quad E\frac{dN_\gamma}{d^4x\, d^3q} \propto T^2 \exp\left\{-\frac{q\cdot u}{T}\right\} \log\left[1+\frac{\kappa(q\cdot u)}{\alpha_s T}\right], \tag{1}$$

where Q (q) is the virtual (real) photon's 4-momentum; effects of a finite chemical potential μ can be absorbed in an additional normalization factor. Note the necessary occurrence of the medium's 4-velocity u to build up Lorentz-invariant rates.

To reduce the number of parameters in the space-time integration, we replace in (1) $T(t,\vec{x}) \to \langle T\rangle \equiv T_{\rm eff}$, $u(t,\vec{x}) \to \langle u\rangle$ and $\int dt\, d^3x \to \int dt V(t) \to N_{\rm eff}$ yielding

$$\frac{dN_{\gamma *}}{d^4Q} \propto N_{\rm eff} \exp\left\{-\frac{M_\perp \cosh(Y-Y_{\rm cms})}{T_{\rm eff}}\right\}, \quad E\frac{dN_\gamma}{d^3q} \propto N_{\rm eff} \int \cdots \exp\left\{-\frac{q_\perp \cosh y}{T_{\rm eff}} \cdots\right\} \tag{2}$$

thus not relying on a particular model for $T(t,\vec{x})$, $u(t,\vec{x})$ and $\mu(t,\vec{x})$ (for the explicit form of (2) cf. [8,9]). This approach is in the spirit of the usual parameterization of the transverse momentum spectra of hadrons by an exponential with a slope parameter and a normalization factor. As an example we show in Figure 1 our results for the invariant mass spectra of dileptons and the momentum spectrum of photons for the experiments of group (i) (cf. [8,9] for more details). Also the transverse momentum spectra of dileptons are described very well [9]. The NA50 acceptance is incorporated only in an approximate way here; the use of the correct filter reproduces the data perfectly [10].

A comparison of our model with the preliminary CERES data [14] of the experiment group (ii) is shown in Figure 2 for $T_{\rm eff} = 145$ MeV and a fairly large value of $N_{\rm eff}$.[3]

Since the experiments of group (iii) cover a large rapidity range an additional Gaussian smearing of the source in (2) needs to be included [9]. In Figure 3 the strength distributions of the thermal dilepton source without and with smearing are displayed. As shown in [9] the shape of the spectra can be well described by $T_{\rm eff} = 160 \cdots 170$ MeV, however, different

[3]Smaller values of $T_{\rm eff}$ deliver a better description of the spectral shape but need even larger $N_{\rm eff}$.

values of $N_{\rm eff}$ are needed. This might be attributed to an inadequate rapidity distribution of our thermal source and different centrality selections in the experiments.

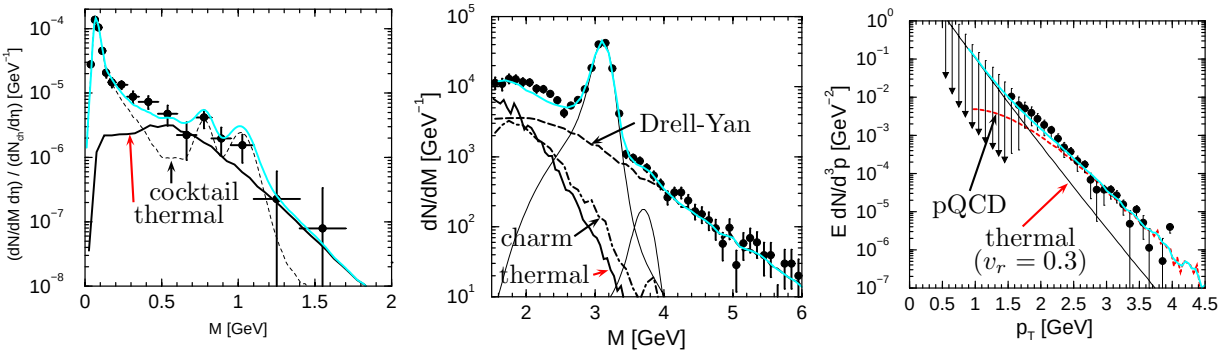

Figure 1. Comparison of our model with dilepton data (left panel for the CERES data [11]; middle panel for the NA50 data [12], thin lines: parameterizations of the J/ψ and ψ') and the photon data (right panel for WA98 data [13]; hadron decay contributions are subtracted). The thermal contribution is characterized by the unique set of parameters $T_{\rm eff} = 170$ MeV and $N_{\rm eff} = 3.3 \times 10^4$ fm^4. Sum of all contributions: gray curves.

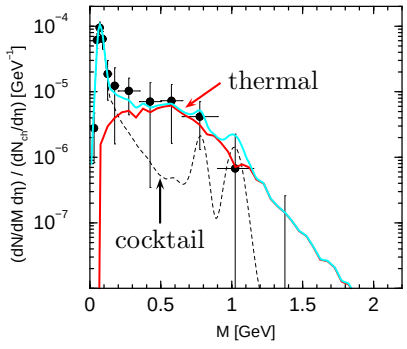

Figure 2. Comparison of our model with preliminary CERES data [14] of the lead beam run at 40 A·GeV.

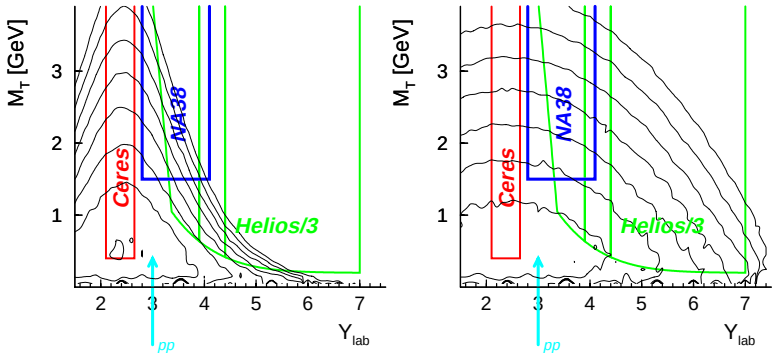

Figure 3. Contour plots of the thermal dilepton distribution in rapidity vs. transverse mass space without (left panel) and with (right panel) smearing in rapidity space for $T = 160$ MeV.

2.2. Time evolution effects

By using a model for $T(t)$ and $V(t)$ and neglecting spatial gradients one can equally well describe the dilepton spectra of the CERES and NA50 collaborations. As shown in [15], there is virtually no difference with the results displayed in Figure 1. The needed initial temperature is 210 MeV, for a given freeze-out temperature of 120 MeV.

2.3. Background contributions

While the analysis of the low-mass dileptons uses a hadronic cocktail and is normalized to the mean multiplicity of charged hadrons, the analyses of the intermediate-mass dileptons and photons need careful estimates of the hard Drell-Yan-like yields and the open charm contribution. We used the PYTHIA event generator with charm quark mass of 1.5

GeV, intrinsic parton transverse momentum distribution width of 0.8 GeV and photon cut-off parameter of 1 GeV. The parameter adjustments are done by comparing with pp and pA data, and then scaling to heavy-ion collisions. The possible subtleties of this procedure are described in [9,16].

3. CONCLUSIONS

In summary we have demonstrated that the superposition of background contributions and a thermal source of real and virtual photons describes the shape of all data from central heavy-ion collisions at CERN-SPS. We find evidence for a large and long-lived thermal source in lead beam experiments at 158 A·GeV. The normalization factor $N_{\rm eff}$ translates into a lifetime of 23 fm/c, in accordance with [17], when assuming a spatial volume of the fireball 1440 fm^3 as found for a radius of 7 fm. The space-time averaged temperature of $T_{\rm eff} = 170$ MeV coincides with both the confinement temperature and the temperature needed to describe the hadron multiplicity ratios in thermal models. Using a model for the temperature and volume evolution of the fireball we find a maximum temperature of 210 MeV indicating an initial state in the deconfinement region. The sulfur beam data point to a similar value of $T_{\rm eff} = 160$ MeV, while the recent preliminary lead beam data at 40 A·GeV can be described by $T_{\rm eff} \leq 145$ MeV.

The present analysis strategy needs to be extended to understand the centrality dependence of the intermediate-mass dileptons as measured by the NA38/50 collaborations [10]. The results of the high-statistic data sampling of dileptons in the lead beam induced reactions at 158 A·GeV by the CERES collaboration is eagerly waited for to decide whether a smooth $q\bar{q}$-like rate is still sufficient. We used it here as a convenient parameterization, and this is not a substitute to a more detailed microscopic calculation.

The consistent description of the real and virtual photon data makes an interpretation of the NA50 data by an anomalous open charm enhancement unlikely. Nevertheless, the explicit measurement of the charm yield, as envisaged by the NA60 collaboration, is needed to arrive at a better understanding of the various dilepton sources.

REFERENCES

1. A. Peshier, B. Kämpfer, O.P. Pavlenko, G. Soff, Phys. Rev. D 54 (1996) 2399, A. Peshier, B. Kämpfer, G. Soff, Phys. Rev. C 61 (2000) 045203.
2. P. Aurenche, F. Gelis, R. Kobes, H. Zaraket, Phys. Rev. D 60 (1999) 076002.
3. K. Gallmeister, B. Kämpfer, O.P. Pavlenko, Prog. Part. Nucl. Phys. 42 (1999) 333.
4. J. Kapusta, P. Lichard, D. Seibert, Phys. Rev. D 44 (1991) 2774.
5. G.Q. Li, C. Gale, Phys. Rev. C 58 (1998) 2914, Phys. Rev. Lett. 81 (1998) 1572.
6. Z. Huang, Phys. Lett. B 361 (1995) 131.
7. R. Rapp, J. Wambach, hep-ph/9909229, Adv. Nucl. Phys., in press.
8. K. Gallmeister, B. Kämpfer, O.P. Pavlenko, Phys. Rev. C 62 (2000) 057901.
9. K. Gallmeister, B. Kämpfer, O.P. Pavlenko, C. Gale, hep-ph/0010332, Nucl. Phys. A, in press.
10. L. Capelli (NA50), this volume; Ph.D. thesis, Univ. de Lyon 2001.
11. B. Lenkeit (CERES), Nucl. Phys. A 661 (1999) 23c; Ph.D. thesis, Heidelberg 1998.
12. E. Scomparin (NA50), Nucl. Phys. A 610 (1996) 331c, J. Phys. G 25 (1999) 235c.

13. M.M. Aggarwal et al. (WA98), Phys. Rev. Lett. 85 (2000) 3595.
14. S. Damjanovic, K. Filimonov (CERES), poster P084 at QM2001.
15. K. Gallmeister, B. Kämpfer, O.P. Pavlenko, Phys. Lett. B 473 (2000) 20.
16. K.O. Gallmeister, Ph.D. thesis, TU Dresden 2001.
17. C.M. Hung, E.V. Shuryak, Phys. Rev. C 57 (1998) 1891.